ELSEVIER

Journal of Structural Geology 30 (2008) 548–564

JOURNAL OF STRUCTURAL GEOLOGY

www.elsevier.com/locate/jsg

Evolving mechanical stratigraphy during detachment folding

Michael Hayes [a], Catherine L. Hanks [b,*]

[a] *Teck Pogo, Inc., P.O. Box 145, Delta Junction, AK 99737, USA*

[b] *Geophysical Institute and Department of Petroleum Engineering, University of Alaska—Fairbanks, Fairbanks, AK 99775, USA*

Received 29 August 2007; received in revised form 9 January 2008; accepted 11 January 2008

Available online 18 January 2008

Abstract

The combination of a complex lithostratigraphy and shortening can lead to a mechanical stratigraphy that changes character and mode of deformation during detachment folding. In the detachment-folded carbonates of the Carboniferous Lisburne Group of northern Alaska, a complex lithostragraphy led to a mechanical stratigraphy that evolved during folding, with mechanical unit thickness decreasing as deformation progressed and the fold tightened. Newly forming mechanical boundaries changed the dominant deformation behavior and subsequent geometry during folding of a given horizon. During early folding, flexural slip dominated in units comprised of thick bedded, competent lithologies while flexural flow dominated in units composed of thinner bedded, incompetent lithologies. After fold ''lock-up'' homogeneous flattening dominated in the less competent mechanical units. The final result was a fold with a complex geometry and a suite of fractures and other structures indicative of both flexural slip/flexural flow folding and homogeneous flattening.

Keywords: Detachment fold; Mechanical stratigraphy; Flexural slip folding; Fractures; Northern Alaska; Lisburne Group

1. Introduction

A detachment fold develops as a result of shortening above a bedding-parallel thrust fault and commonly forms in mechanically layered strata, where a relatively competent unit (e.g., limestone) overlies a relatively incompetent unit (e.g., shale) (Fig. 1; Jamison, 1987). Thus the evolution of a detachment fold and its final geometry are controlled in large part by this contrast in relative competency.

The term ''mechanical stratigraphy'' refers to the way a sequence of rocks responds to deformation, occurs at a variety of scales (e.g., Latta and Anastasio, 2007), and is a result of different compositions, competencies, bed thicknesses, interface strengths, and anisotropies (Ladeira and Price, 1981; Ramsay and Huber, 1987; Tanner, 1989; Narr and Suppe, 1991; Fischer and Jackson, 1999). These mechanical properties have a direct influence on the deformational style of individual layers as well as the entire stratigraphic package. Mechanical stratigraphy can also change during deformation in response to changing environmental factors (e.g., temperature, pressure, and fluids) (Fischer and Jackson, 1999).

In many mechanical and geometric models of detachment folds, the mechanical stratigraphy is a relatively simple, two-layer system that stays constant throughout deformation (Fig. 1; Epard and Groshong, 1995; Homza and Wallace, 1995, 1997; Poblet and McClay, 1996; Atkinson and Wallace, 2003). However, many lithostratigraphic packages are quite complex, consist of multiple layers with different mechanical properties, and have deformational responses that change with varying temperatures, strain or structural position (e.g., Gutierrez-Alonso and Gross, 1999; Latta and Anastasio, 2007). The way each mechanical unit responds to shortening during folding is reflected in the mesoscopic and microscopic structures that form.

In this study, we document the distribution of fractures and other structures and their relationship to both deformation behavior and mechanical stratigraphy in a detachment fold in the Carboniferous Lisburne Limestone of northern Alaska. We then develop a model for the evolution of the fold that is directly related to the mechanical stratigraphy. The study

* Corresponding author. Tel.: +1 907 474 5562; fax: +1 907 474 5163.
E-mail address: chanks@gi.alaska.edu (C.L. Hanks).

0191-8141/$ - see front matter © 2008 Elsevier Ltd. All rights reserved.
doi:10.1016/j.jsg.2008.01.006

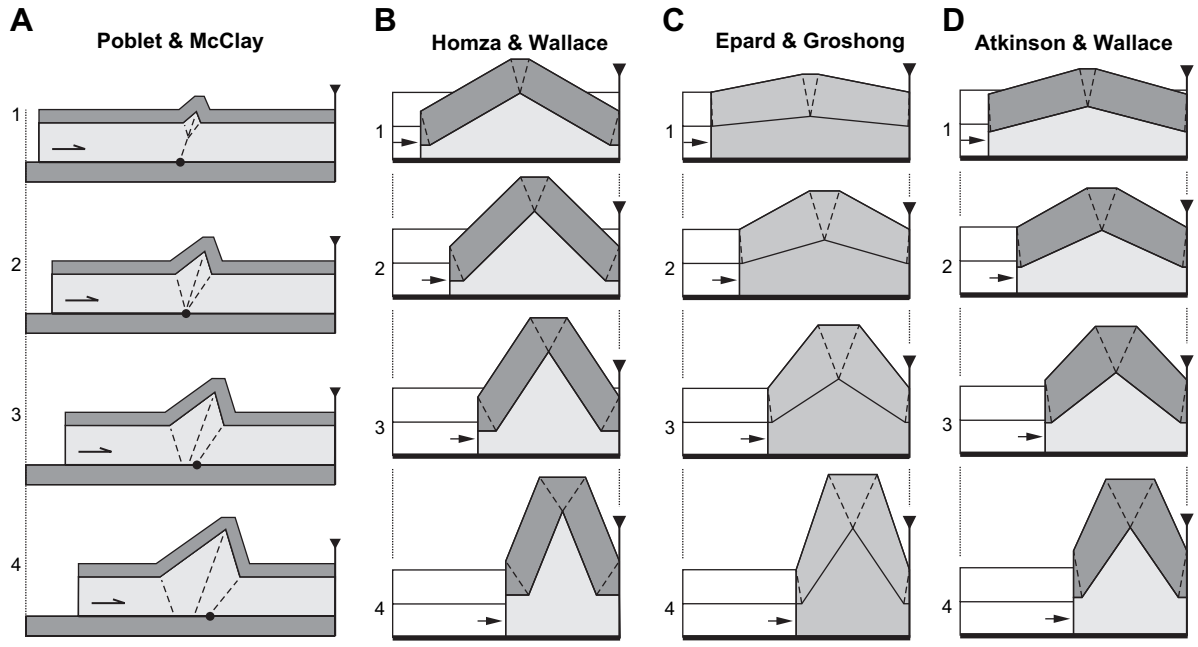

Fig. 1. Four models for the evolution of detachment folds. Detachment units are light gray, competent units are dark gray. (A) Poblet and McClay, "Model 1" (migrating hinges); (B) Homza and Wallace; (C) Epard and Groshong (Note that no distinction is made between the incompetent detachment horizon and competent horizon); (D) Atkinson and Wallace (variation of the Homza and Wallace model that allows thickening of the competent unit similar to the Epard and Groshong model). Modified from Poblet and McClay, 1996; Atkinson, 2001; Atkinson and Wallace, 2003; Shackleton, 2003.

illustrates that mechanical stratigraphy is not a static characteristic and can change character during folding, profoundly influencing the resulting fold geometry and kinematics.

2. Geologic setting

2.1. Structure and lithostratigraphy

The Brooks Range is the northern structural continuation of the backarc fold-and-thrust belt of the Cordilleran orogen (Fig. 2). In Alaska, collision of an island arc resulted in the collapse of a south-facing Paleozoic passive continental margin (Moore et al., 1994). Most shortening occurred during Late Jurassic to Early Cretaceous time (Moore et al., 1994). Episodic post-collisional contraction during the Cenozoic caused a northward progradation of the fold-and-thrust belt and formation of the northeastern Brooks Range (Wallace and Hanks, 1990).

The stratigraphy of the northeastern Brooks Range has three distinct depositional sequences (Fig. 3; Bird and Molenaar, 1987; Moore et al., 1994). The pre-Mississippian sequence consists of slightly metamorphosed and strongly deformed sedimentary and volcanic rocks of Proterozoic to Devonian age. It is unconformably overlain by Mississippian to Lower Cretaceous northerly-derived passive margin clastic and carbonate rocks of the Ellesmerian sequence. The overlying Brookian sequence consists of Lower Cretaceous to Recent clastic rocks derived from the Brooks Range to the south (Moore et al., 1994).

The structural style of the northeastern Brooks Range is dominated by anticlinoria cored by sub-Mississippian rocks (Figs. 4 and 5) that are interpreted to be horses in a regional north-vergent duplex with a floor thrust in the pre-Mississippian sequence and a roof thrust in the incompetent Mississippian Kayak shale (Wallace and Hanks, 1990). Shortening above the duplex is accommodated primarily by detachment folding of the competent Mississippian through Triassic rocks (Wallace and Hanks, 1990). The Carboniferous Lisburne Group is the most competent member of the roof sequence and deforms predominantly into second-order kilometer-scale, east-west trending, symmetrical detachment folds (Fig. 5) (Wallace, 1993). Third-order folds in the lower Lisburne have wavelengths of ~30–500 m (Fig. 5 inset) and contribute to thickening of the second-order folds hinges.

A third-order detachment fold within the lower Lisburne is the focus of this study. It is located on the northern crest of the Echooka anticlinorium (Figs. 4–6) and is a typical, albeit very well exposed, example of a Lisburne detachment fold.

2.2. Mechanical stratigraphy

The definition of mechanical stratigraphic units is scale-dependent (Fischer and Jackson, 1999; Latta and Anastasio, 2007). Four regional mechanical units are relevant to the stratigraphy and structures described in this paper (Fig. 3) and include: (a) the competent pre-Mississippian sequence and Kekiktuk Conglomerate, (b) the incompetent Kayak Shale, (c) the competent Lisburne Group and Echooka Formation, and (d) the incompetent Kavik Shale (Wallace and Hanks, 1990; Wallace, 1993; Atkinson and Wallace, 2003).

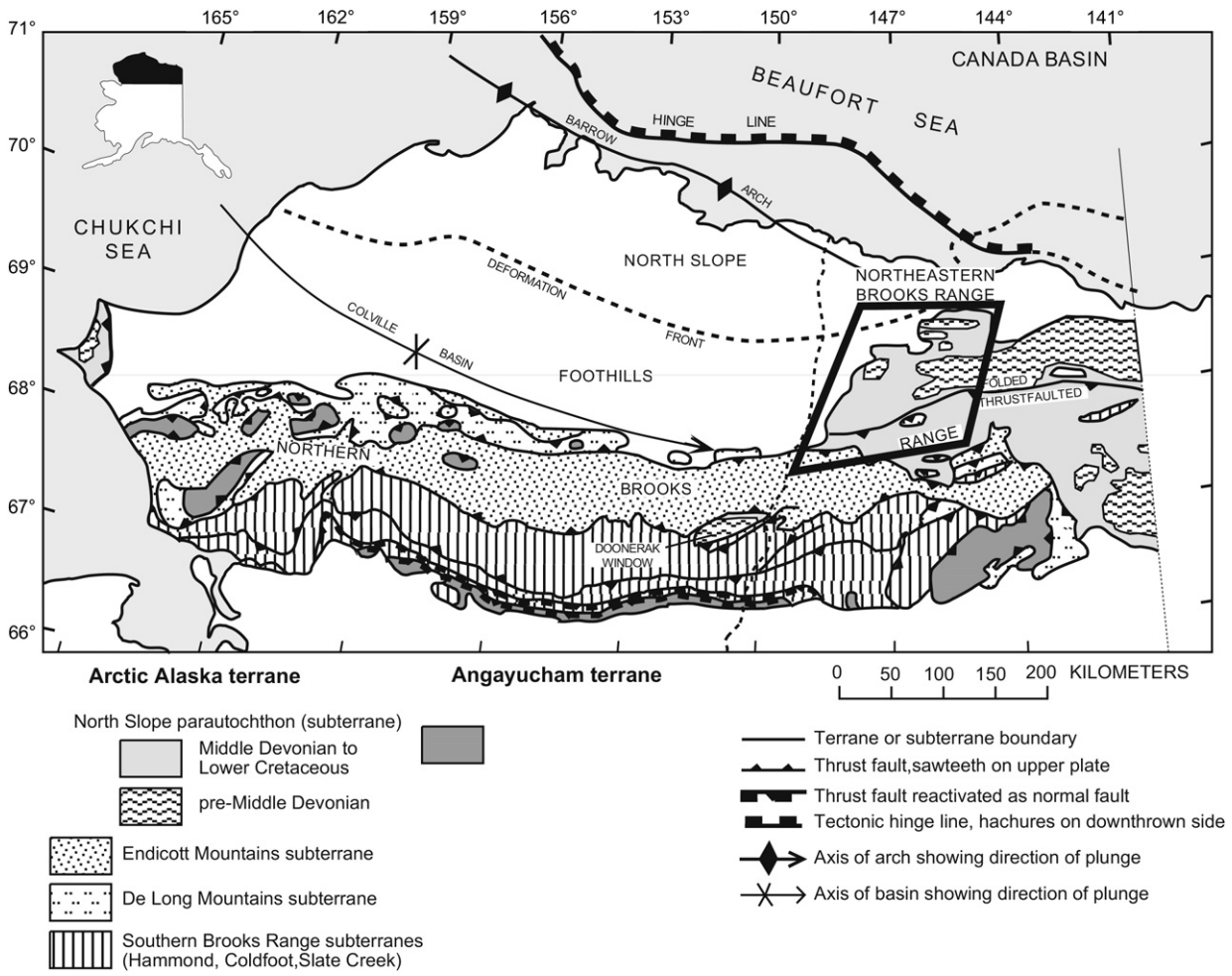

Fig. 2. Regional structure and tectonic map of the Brooks Range and North Slope of Alaska. Outlined area is shown in Fig. 4. Modified from Moore et al., 1994.

Although commonly described as a single mechanical layer at the regional scale, the Lisburne Group is not mechanically homogenous throughout its ~500 m thickness. It consists of four separate mechanical subunits (Fig. 3) (Wallace, 2001; Atkinson and Wallace, 2003): (1) The lower Alapah: alternating strong and weak, decimeter-scale beds of shale and limestone with well-defined slip surfaces and is relatively incompetent; (2) the upper Alapah: decimeter- and meter-scale limestone beds with less well-defined slip surfaces, but is relative competent; (3) the lower Wahoo: meter-scale limestone beds with poorly defined slip surfaces, and is the most competent; and (4) the upper Wahoo: decimeter-scale limestone beds similar in competency to the lower Alapah.

3. Definition of detailed mechanical stratigraphy

Mechanical units were defined and characterized within the fold based on field examination of structural style and character (Fig. 6, Table 1). A mechanical unit was defined as an individual bed or a package of beds with common mechanical characteristics, including gross lithologic character, average bed thickness, presence of slip horizons, and overall mesoscopic and microscopic deformation style. Bed surfaces were identified as slip horizons if they had slickenlines and/or slickenfibers or if bed-perpendicular, calcite-filled fractures were laterally offset along them. Slip direction was determined using slickenfiber steps and lateral offset of filled fractures. Slip magnitude was fairly speculative due to difficulty determining which offset vein segments matched across the bedding-slip surface.

Fracture sets were distinguished based on orientation and presence of mineral fill (primarily calcite). The relative ages of the fractures were determined by crosscutting and abutting relationships. To determine fracture density for each fracture set, scan-line surveys were conducted for each set within each mechanical unit. Where exposure and accessibility allowed, surveys were conducted in multiple structural positions (north limb, south limb, and hinge) within a single mechanical unit.

Carbonate lithologies involved in this fold include carbonate mudstone, wackestone, and packstone. Mechanical units were considered ‘‘competent’’ if they consist of coarse-grained lithologies, were dominated by fractures and had discrete internal slip horizons. Units consisting of finer-grained lithologies dominated by spaced cleavage and/or penetrative strain and/or distributed layer-parallel shear structures were considered ‘‘incompetent.’’ In general, muddy layers were incompetent with peloidal mudstones less competent than micritic mudstones. Calcareous shale beds <10 cm thick were

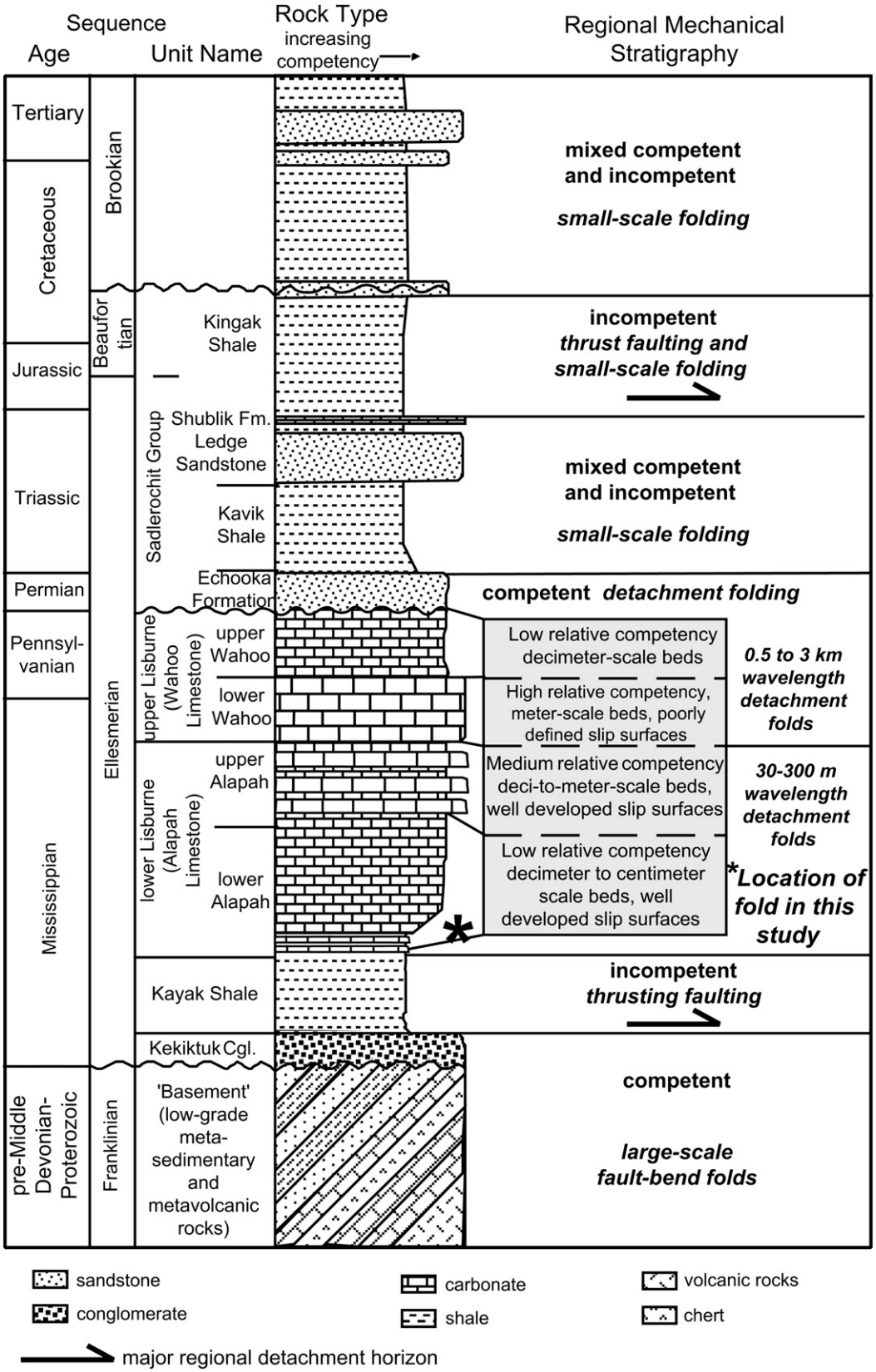

Fig. 3. The regional lithostratigraphy and mechanical stratigraphy of the northeastern Brooks Range. Based on Bird and Molenaar, 1987; LePain, 1993; and modified from Brinton, 2002.

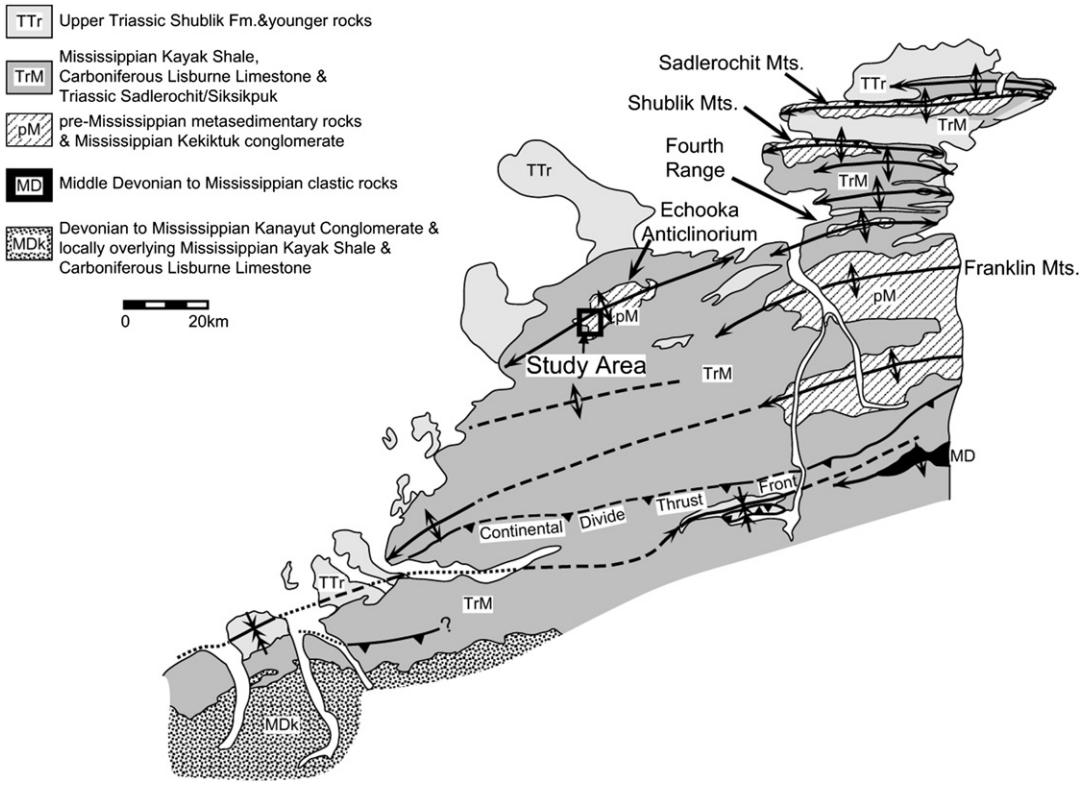

Fig. 4. Geologic map of the western part of the northeastern Brooks Range, showing the location of the Echooka anticlinorium and the fold discussed in this paper. Modified from Hanks et al., 2004.

occasionally interbedded within carbonate lithologies and commonly coincided with mechanical unit boundaries.

4. Observations

4.1. Mechanical stratigraphy and fold geometry

The detachment fold is a symmetric, non-cylindrical fold with a wavelength of ~150 m and an interlimb angle of 90–115° (Fig. 6). The interlimb angle and fold shape change up-section along a gently curved hinge surface.

Three geometrically distinct, larger-scale mechanical units can be identified based on changes in unit thickness and overall structural geometry (Fig. 6B, Units 1–3). Each of these mechanical units can be further subdivided into subunits based on the presence of slip horizons and the character and distribution of mesoscopic and microscopic structures (Figs. 6B and 7, subunits a–m).

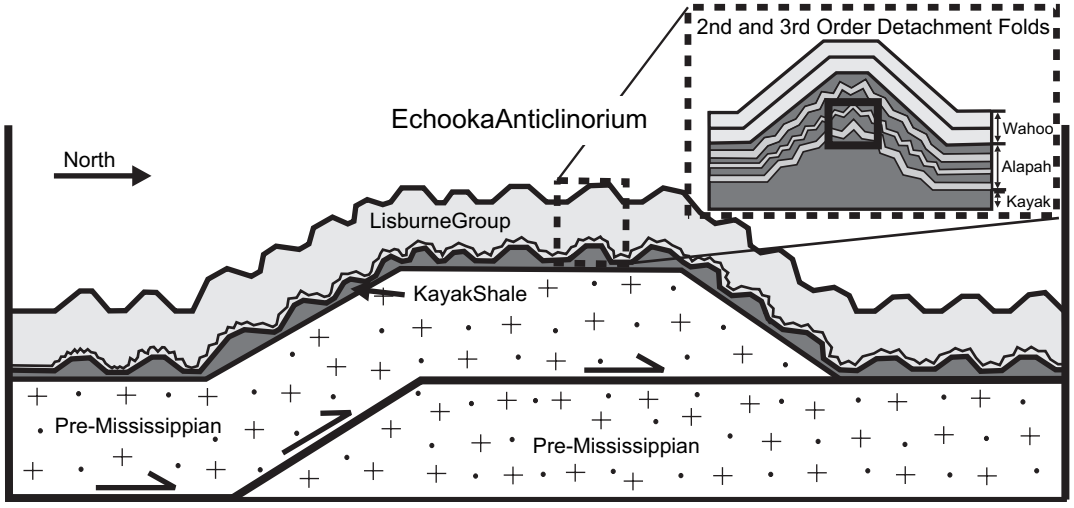

Fig. 5. A schematic cross section of the western part of the northeastern Brooks Range, illustrating the three orders of folding in the Lisburne Group and the location of the third-order fold examined in this study. Dashed box shows the location of the studied fold with respect to the regional anticlinoria; solid inset box depicts the approximate location of the studied fold with respect to the second-order fold. Modified from Brinton, 2002.

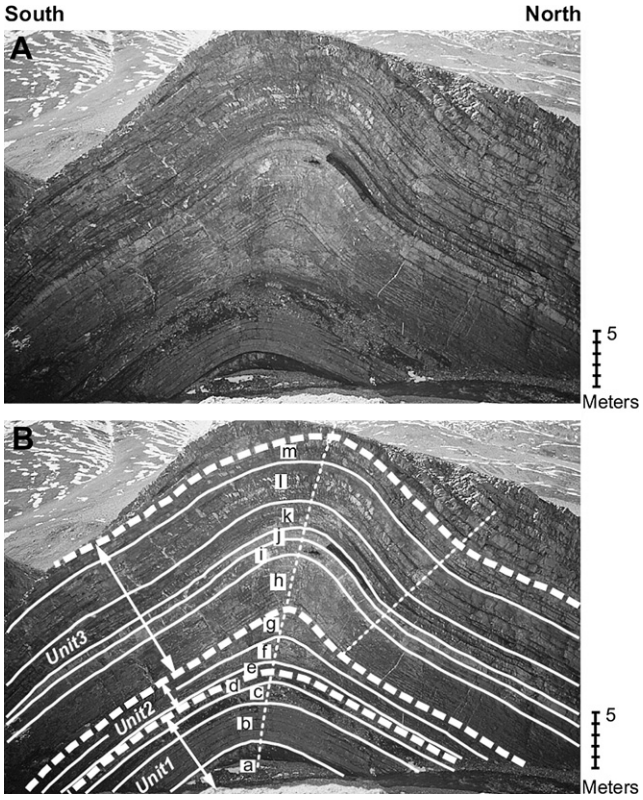

Fig. 6. (A) Photograph looking east showing the exposure and geometry of the detachment fold discussed in this paper. (B) Photograph of fold with mechanical Units 1–3 and subunits a-m defined. Note the thickness change in Unit 2 and the bifurcating synclinal hinge in Unit 3 of the north limb. The dotted lines represent the hinge surfaces.

The structurally lowest mechanical unit, Unit 1, shows no change in unit thickness from limb to hinge and fold geometry (or shape) is rounded with an interlimb angle of 115° (Figs. 6B and 8A). Unit 1 can be further subdivided into subunits a–d (Figs. 6B and 8A). These subunits consist primarily of moderate to thick (0.6–1.4 m) beds of bioclastic packstone and wackestone with widely spaced slip horizons.

In contrast, mechanical Unit 2 shows a distinct increase in thickness from limb to hinge (Figs. 6B and 8B) and a corresponding change in fold shape, with a decrease in the fold interlimb angle from 115° to 90°. The three subunits that compose Unit 2, e–g, consist primarily of thinly bedded mudstones (0.1–0.6 m) with closely spaced slip horizons. These subunits show a progressive increase in percentage thickness change from bottom to top (Table 2).

Mechanical Unit 3 shows no change in unit thickness from limb to hinge and fold geometry is sub-rounded to rounded (Figs. 6B and 8C,D) with an interlimb angle of 90°. Unit 3 is also deformed by a syncline that does not affect either of the underlying units. The synclinal hinge bifurcates upward from the north limb of the anticline and has an interlimb angle of ~160° (Fig. 6B). The mechanical subunits within Unit 3 (h–m) consists primarily of evenly bedded (0.5–0.8 m) packstones with widely spaced slip horizons.

4.2. Fractures

Fractures, both filled and unfilled, are the most abundant mesoscopic structure. Four distinct fracture sets were distinguished based on orientation, presence or lack of vein material, and mutual age relationships (Table 3). The oldest fracture set is referred to as Set 1; the youngest as Set 4. Most fractures were assumed to be primarily extensional in nature (Mode 1) because of the presence of plumose ornamentation and/or the lack of wall-parallel offset.

4.2.1. Set 1 fractures

Set 1 fractures strike north-northwest, perpendicular to the fold hinge. These fractures are planar, steeply dipping and subperpendicular to bedding and terminate within beds. The fractures are filled with coarse calcite with no evidence of wall-parallel shear. Fracture spacing varies between mechanical subunit, with an average spacing of <15 cm in each unit (Table 4) and increases with greater average bed thickness and mechanical unit thickness.

4.2.2. Set 2 fractures

Set 2 fractures are west-northwest striking and oblique to subparallel to the fold hinge. These fractures are calcite-filled, planar extension fractures. Dip is variable, with dips perpendicular, oblique and parallel to bedding all observed. The bedding-parallel set 2 fractures have multiple crack-seal textures. Apertures for set 2 fractures range from hairline (<1 mm) to 9 cm. These fractures are grouped as a single set because they have a similar strike, are calcite filled and have no consistent relative age relationship. Collectively they are the second oldest set.

In thick mechanical subunits that consist of multiple thin beds (e.g., subunits b, h, k, l, and m), most set 2 fractures cut through several beds, and terminate within bedding and within the mechanical subunit (Table 3). In the few mechanical subunits that consist of single beds (e.g., subunit d), set 2 fractures are confined to and terminate within that bed. These observations suggest that Set 2 fracture propagation is not limited by lithologic heterogeneity.

Several large, late set 2 fractures also cut multiple mechanical units in Fold 1, including a single fracture that cuts across the entire exposed thickness in the northern limb of the fold (Fig. 8). These large fractures are either present in swarms with a range of apertures (2–30 mm) or are widely spaced with large apertures (20–90 mm). They are oriented sub-perpendicular to bedding, and clearly post-date the set 2 fractures discussed above. In the less competent mudstone and shale beds, these large set 2 fractures are sheared top to north in the southern limb and top to south in the northern limb (Fig. 8B). A limited amount of bed-parallel offset across bedding-slip surfaces (<10 cm) of these larger fractures has occurred along slip horizons between most of the mechanical subunits.

Table 1
Characteristics of mechanical units

Unit	Subunit	Lithology	Fracture sets observed	Locations and character of slip horizons	Deformational features observed
3	m	Bioclastic packstone	Sets 1 2, 3 & 4	Lower and upper contacts	Dissolution seams and strongly sutured fabric; bioclasts have planar calcite twins
	l	Bioclastic peloidal packstone	Sets 1 2, 3 & 4	Lower and upper contacts; additional horizon ~midway through unit	Dissolution seams; sutured fabric; stylolitic horizon; flattened peloids
	k	Mudstone & calcareous shale	Sets 1 2, 3 & 4	Both lower and upper contacts; 2 additional internal horizons in shale beds	Dissolution seams perpendicular to bedding; sutured fabric; planar calcite twins in set 1 and 2 fracture fill
	j	Micritic mudstone & calcareous shale	Sets 3 & 4	Upper contact with unit k	Very closely spaced unfilled set 3 and 4 fractures
	i	Bioclastic packstone & calcareous shale	Sets 1 2, 3 & 4	In the south limb of fold, between the top two beds of i	Plumose marks on set 4 fracture faces; anastomosing dissolution seams; bed parallel stylolites
	h	Bioclastic packstone	Sets 1 2, 3 & 4	In 10 cm shale bed between units h and i	Plumose marks on set 4 fracture faces; anastomosing dissolution seams; bed parallel stylolitic horizons; en echelon bed perpendicular set 2 fractures
2	g	Mudstone	Sets 1 2 & 3	Upper contact with unit h (only observed on south limb with top to north offset)	Cleavage sub-parallel to axial surface and divergent downward from the hinge
	f	Peloidal mudstone	Sets 1 2, 3 & 4	Multiple closely spaced (~5 cm) slip horizons within unit f. Several slip horizons contain layer-parallel calcite filled fractures	Plumose marks on set 3 and 4 fracture surfaces; dissolution seams and cleavage sub-parallel to axial surface and divergent downward from the hinge and cross-cut set 2 fractures; flattened peloids; folded, rotated, and extended layer-parallel calcite filled fractures; boudinage of bedding
	e	Wackestone mudstone	Set 2	Lower contact with unit d	Cleavage sub-parallel to axial surface and divergent downward from the hinge; asymmetric stylolites
1	d	Peloidal packstone	Sets 2, 3 & 4	Upper contact with unit e; has calcite fill with crack-seal laminae	Dissolution seams oriented perpendicular to bedding. Flattened peloids with S1 oriented perpendicular to bedding
	c	Bioclastic packstone & calcareous shale	Sets 3 & 4	None	Dissolution seams and slatey cleavage at a low-angle to bedding (divergent downward from hinge)
	b	Bioclastic wackestone	Sets 1 2, 3 & 4	Two horizons at and near the base of the unit with top to north kinematic indicators	Plumose marks on set 3 and 4 fracture surfaces. Dissolution seams sub-perpendicular to bedding
	a	Bioclastic mudstone with shale bed at upper contact	Sets 1 & 2	Upper contact with unit b on south side of hinge. Has calcite fill with crack-seal laminae	Non-penetrative dissolution seams perpendicular to bedding. Bedding-parallel foliation within the shale bed

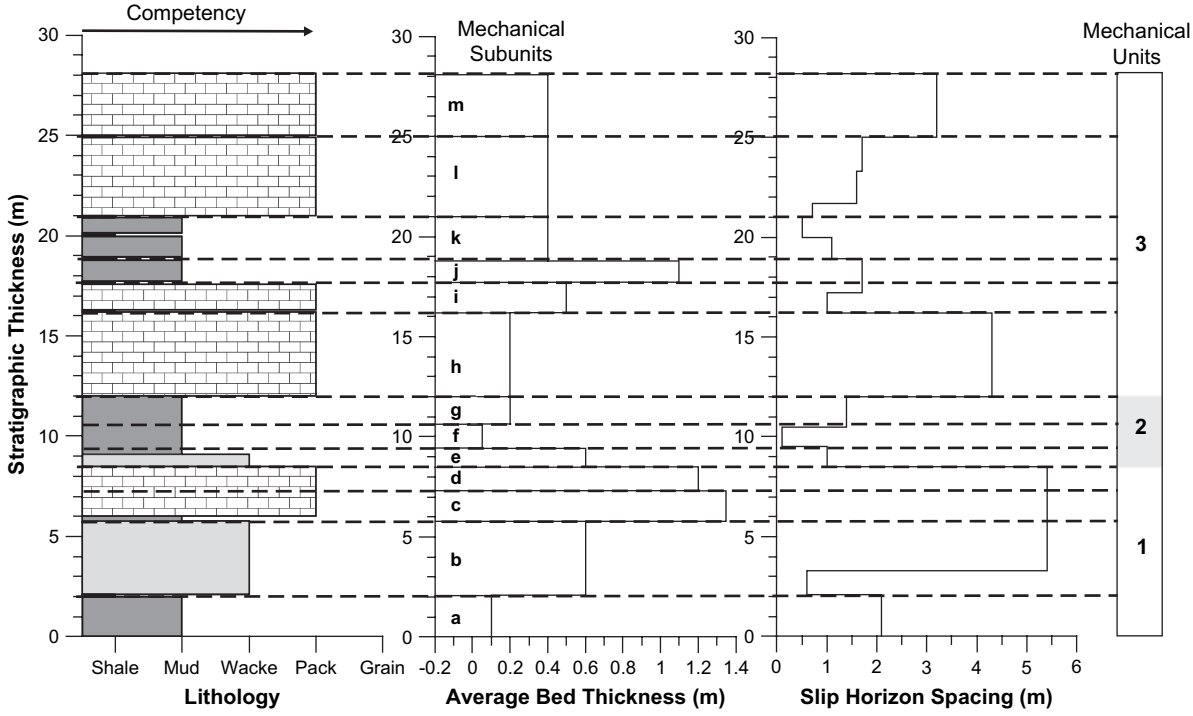

Fig. 7. Lithology, average bed thickness, and slip horizon spacing throughout the surveyed stratigraphic thickness of the studied fold. Dashed lines are the mechanical subunit boundaries, (labeled a–m in the average bed thickness column). Relative competency increases from shale to packstone.

4.2.3. Set 3 character and distribution

Set 3 fractures are west-northwest to west-southwest striking, oblique to subparallel to the fold hinge, and sub-perpendicular to bedding (Table 3). Fractures dip steeply with north dips in the southern limb of the fold and south dips in the northern limb. The fractures are planar to anastomosing and unfilled. Plumose ornamentation on set 3 fracture surfaces and a lack of evidence for wall-parallel shear suggest that these are extensional (Mode 1) fractures. Most set 3 fractures terminate at bedding contacts, thin shale beds or against other set 3 fractures (Table 4), which implies that bed thickness limits the size and spacing of these fractures.

The unfilled set 3 fractures clearly post-date the filled fractures of sets 1 and 2. The majority of set 3 fractures predate set 4 fractures, but in some locations the age relationship is ambiguous.

4.2.4. Set 4 character and distribution

Set 4 fractures are north-northwest striking, subvertical, vertically extensive and unfilled (Table 3). Plumose ornamentation on many set 4 fractures suggests they are extension (Mode 1) fractures. Many set 4 fractures cross several mechanical unit boundaries, suggesting that they are not constrained by either lithologic bedding or mechanical units.

4.3. Other structures

A variety of other mesoscopic and microscopic structures are observed throughout the fold (Figs. 8 and 9). Mesoscopic structures resulting from shortening include spaced cleavage and parasitic folding of set 2 fractures. Cleavage is limited to less competent mudstone subunits e, f, and g (Fig. 9B), and thin interbedded shale layers (e.g., lower bed in subunit c, Fig. 8A). Cleavage is oriented parallel to the hinge surface, is most pervasive in the hinge area and diverges away from the fold core. In several thin shale layers, the cleavage is subparallel to bedding in both the north and south limbs. Bedding-parallel, calcite-filled set 2 fractures are folded into small-scale parasitic folds in the fold hinge (Figs. 8B and 9A). The axial planes of these parasitic folds parallel the hinge plane of the host fold.

Microscopic structures indicative of pervasive shortening are present in most lithologies. Dissolution seams occur in most mechanical units and are oriented sub-parallel to the hinge surface and perpendicular to bedding (Fig. 9B). Sutured clast boundaries are common in coarser-grained packstones. Flattened clasts are restricted to lithologies with peloids, and have S_1 axes oriented parallel to the hinge surface and/or perpendicular to bedding and S_3 axes oriented approximately north and parallel to bedding.

Bedding and the layer-parallel calcite-filled set 2 fractures in both fold limbs have been boudinaged (Fig. 9C and E). These structures suggest extension of both limbs.

Mesoscopic structures indicating shear include slickenline and slickenfibers on slip surfaces, displacement of fractures parallel to slip horizons, rotation of calcite rhombs and duplexing of bed-parallel Set 2 fractures (Fig. 9D and E). Slickenline and slickenfibers consistently trend $355 \pm 15^\circ$ and are perpendicular to the fold hinge. Calcite rhombs resulting from the boudinage of bed-parallel set 2 fractures are locally rotated,

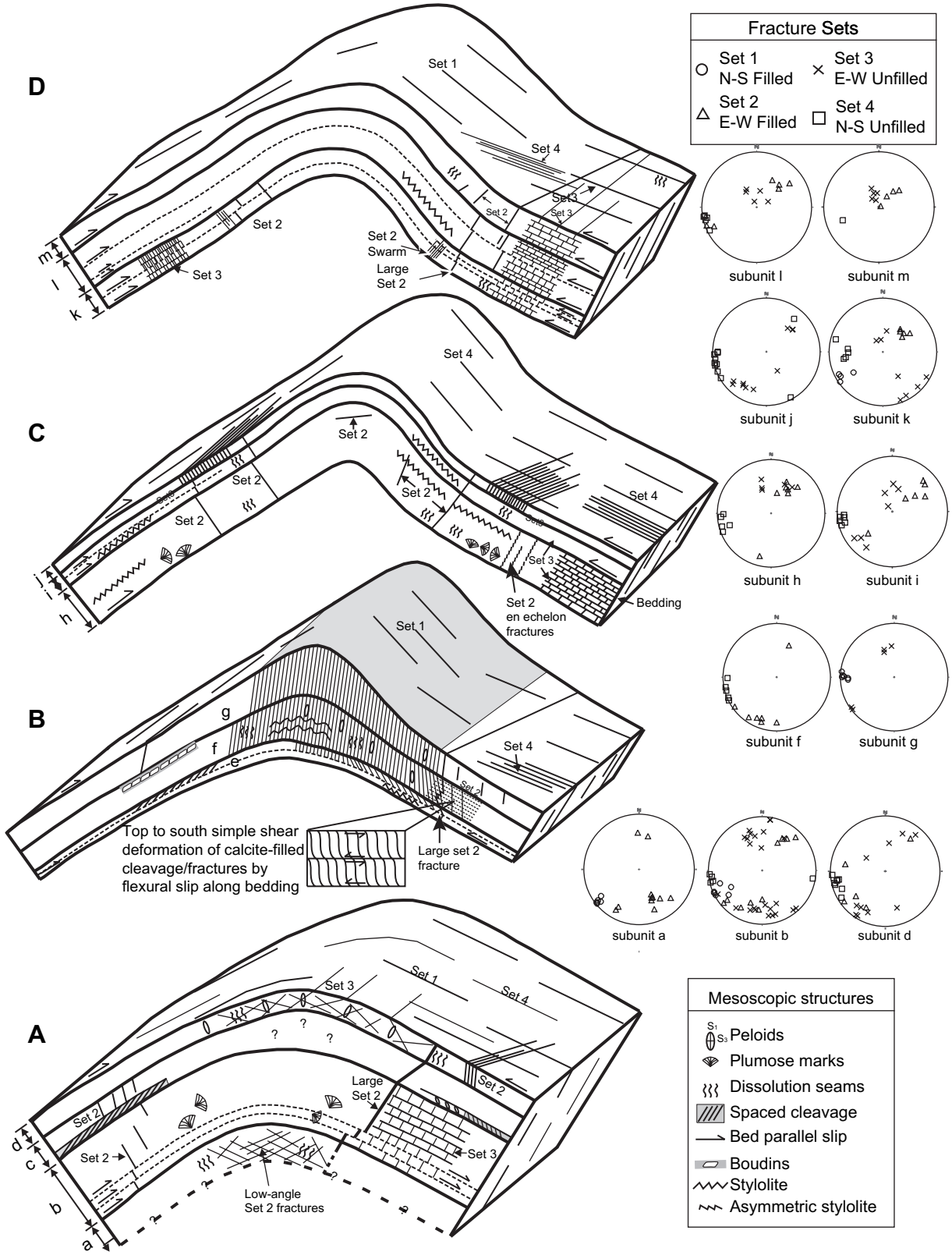

Fig. 8. Character and distribution of observed mesoscopic structures: (A) Unit 1, subunits a–d; (B) Unit 2, subunits e–g; (C) Unit 3, subunits h–j; (D). Unit 3, subunits k–m. Question marks indicate contacts and sections of the fold that were not exposed. Fracture Sets 1 and 2 shown in heavy dark line; Sets 3 and 4 in light lines. The large set 2 fracture cuts through the entire fold. Shaded area in B indicates the horizontal extent of the spaced cleavage inferred along fold strike. Bedding surfaces are pervasive throughout the structure, but are not included for clarity.

Table 2
Subunit thickness, average bed thickness, percentage thickness change from limb to hinge, and interlimb angle of each mechanical subunit

Mechanical unit	Mechanical subunit	Thickness (m)	Ave. bed thickness (m)	Percentage thickness change	Interlimb angle (degrees)
3	m	3.2	0.40	0	93
	l	4	0.40	0	93
	f	1.2	0.40	0	93
	j	1.1	1.10	0	93
	i	1.6	0.50	0	93
	h	4.2	0.20	0	93
2	g	1.4	0.20	100	90
	f	1.2	0.05	83	115–90
	e	0.9	0.60	55	115
1	d	1.2	1.20	0	115
	c	1.5	1.35	N/A	115
	b	3.7	0.60	0	115
	a	2.1	0.10	N/A	115

Subunit thickness measurements are the north limb of the fold. N/A refers to data not available due to limited exposure.

with top-to-north rotation in the south limb and top-to-south rotation in the north limb (Fig. 9D).

Cross-cutting relationships between these structures suggest that some extensional structures preceded development of compressional structures, while other extensional structures post-dated compression. Flexural slip and related shear structures affect both compressional and extensional structures.

5. Interpretation

The fold described in this study is a chevron-style buckle fold involving a heterogeneous, highly layered mechanical stratigraphy. Since mesoscopic structures that develop during folding reflect the response of each mechanical unit to shortening, we use the relative timing and distribution of mesoscopic structures to both define the mechanical stratigraphy and determine the fold evolution (Figs. 8 and 11).

In general, two important deformation behaviors during buckle folding in a layered sequence are flexural slip and flexural flow (Ramsay and Huber, 1987; Tanner, 1989; Davis and Reynolds, 1996). Flexural slip accommodates buckling by layer-parallel slip along discrete surfaces while flexural flow accommodates buckling by distributed layer-parallel flow or shear. In both flexural slip and flexural flow, bed thickness remains constant. During flexural slip or flexural flow, buckling of rigid layers can result in tangential longitudinal strain in the fold hinges (TLS; Ramsay and Huber, 1987; Price and Cosgrove, 1990). For TLS, the outer arc of the rigid layer undergoes layer-parallel lengthening and the inner arc experiences shortening (Fig. 10). Alternatively, extension in the hinge can result in hinge collapse. However, hinge collapse is rarely observed in Lisburne detachment folds (Homza and Wallace, 1995, 1997).

In many buckle fold models, flexural slip ceases at an interlimb angle of ~60° and the fold becomes ''locked'' (Ramsay, 1974; Tanner, 1989; Twiss and Moores, 1992; Yang and Gray, 1994). Additional folding continues via homogeneous flattening, with material flowing from the limbs and into the fold hinge, resulting in a geometric modification of the original fold (Ramsay and Huber, 1987; Ismat and Benford, 2007).

5.1. Mechanical stratigraphy, fold mechanism and geometry

In this particular detachment fold, the fold geometry and the distribution and character of mesoscopic and microscopic

Table 3
The general characteristics of fracture sets 1–4

Fracture set	Fracture orientation	Fracture characteristics
1	NNW striking—perpendicular to fold strike. Dip to east, sub-perpendicular to bedding	Calcite filled, planar, Mode 1 extension fractures. Oldest set observed
2	WNW striking—oblique/sub-parallel to fold strike. Variable dip—perpendicular, parallel, or oblique to bedding	Calcite filled, planar, Mode 1 extension fractures cross-cutting multiple bedding planes. Bedding parallel fractures show multiple crack-seal deformational features
3	WNW–WSW striking—oblique/sub-parallel to fold strike. Dip sub-perpendicular to bedding	Unfilled, planar to anastomosing, Mode 1 extension fractures confined by bedding planes. Third oldest set observed in most locations, but timing relationship with set 4 fractures can be ambiguous
4	NNW striking—perpendicular to fold strike. Dip to east, sub-perpendicular to bedding	Unfilled, planar, Mode 1 extension fractures. Plumose structures on several fracture faces. Youngest fracture set in the most locations

Table 4
Fracture set character and distribution within individual mechanical units. Some units have data for multiple structural positions (e.g. North limb, South limb, Hinge)

Mechanical unit	Ave. spacing (cm)	Aperture (mm)	Ave. height (cm)	Nature of termination
Set 1				
k	14.7	<1 to 5	38	AB, WB
g	1.9	≤1	11.7	WB
f	1.5	≤1	11.1	WB, AB
b	8.1	<1 to 13	51.9	WB
a	6.1	<1 to 2	15.2	WB
Set 2				
m	4.2	<1 to 15	21.8	WB
l	7.9	<1 to 90	44.3	WB, AB, Set 2
k (N limb)	8.4	<1 to 10	19.7	WB, Set 2
i	18.5	<1 to 20	57.3	WB, Set 2
h	6.6	<1 to 10	36.2	WB
f	19.9	<1 to 20	43.6	WB, SS, Set2
d (hinge)	2.9	<1 to 10	12.6	WB
d (N limb)	7.3	<1 to 24	22.1	WB
b	10.7	<1 to 70	28.6	WB, AB, Set 2
a	3.5	<1	23	WB & Set 2
Set 3				
m	21.1	≤1	34.3	AB, WB, Set 3
l	13.5	≤1	28.6	AB, WB, Set 3
k (S limb)	3.8	≤1	32.6	AB, WB
k (N limb)	14.9	≤1	28.3	AB, WB, Set 3
j (S limb)	6	<1	33.2	AB, WB, Set 3
j (N limb)	0.9	<1	11.3	WB
i	7.7	<1 to 2	12.7	SH, WB, Set 3
h	6.9	≤1	20.2	AB, WB
g	13.1	≤1	16.2	AB, WB
f	6	≤1	5	AB
d (hinge)	8.2	≤1	28.6	AB, WB, Set 3
d (N limb)	6.2	<1 to 3	17.5	FPB, AB, WB
b (S limb)	12.5	≤1	19.9	AB, WB, LAF, Set 3
b (N limb to hinge)	13.3	<1 to 2	21.1	AB, WB, LAF
Set 4				
m	3	<1 to 2	24.7	Set 3, Set 4, WB
l	5.6	≤1	27.8	Set 3, WB
k	9.8	<1	30.1	AB, WB, Set 4
j	1.1	<1	9.6	WB
i	5.9	<1 to 2	Ind.	AB
h	3.3	<1 to 2	20	WB, Set 3, Set 1
b	21.7	<1 to 4	12.7	Set 3

If the structural position is not labeled, the data were collected in the north limb. WB, within bedding; AB, at bedding; SS, slip surface at bedding; SH, stylolitic horizon; Set 1, fracture terminates at a set 1 fracture; Set 2, fracture terminates at a set 2 fracture; Set 3, fracture terminates at a set 3 fracture; Set 4, fracture terminates at a set 4 fracture.

structures indicate that both flexural slip and homogeneous flattening were active at some point in the fold history, but not homogenously throughout the fold. The lithostratigraphy can be subdivided into three different mechanical units that responded differently to shortening (Fig. 6).

Unit 1 consists of relatively competent lithologies with sparse and widely spaced slip horizons, and maintains constant bed thickness from fold hinge to limbs. We interpret Unit 1 as having deformed primarily via flexural slip along discrete bedding surfaces and flexural flow within less competent mudstone and shale layers.

Unit 2 consists of mudstone and is incompetent in comparison to the units above and below it. Beds are thin and slip-horizon spacing is small. Layers are significantly thickened in the hinge area, and have structures that indicate early slip along bedding planes. These early-formed shear structures are overprinted by spaced cleavage. Unit 2 is interpreted to have experienced an early stage of buckling by flexural slip and flexural flow with subsequent homogenous flattening. The restriction of homogeneous flattening and associated hinge thickening to Unit 2 resulted in a decrease in the interlimb angle of the overlying units by $\sim 25^{\circ}$.

Like Unit 1, Unit 3 consists of relatively competent lithologies, has an internally consistent fold shape, maintains constant bed thickness from limb to hinge and has no evidence of penetrative strain. Unit 3 is interpreted to have folded by flexural slip and flexural flow.

5.2. Fracture character, timing and relationship to active mechanical stratigraphy and folding

The character of the different fracture sets and their age relative to other mesoscopic structures provide important clues as to which mechanical units were active during folding.

5.2.1. Pre-folding

Set 1 fractures are sparse, vertically extensive, and commonly crossing multiple bed and mechanical boundaries, suggesting that the stratigraphy acted as a single mechanical unit during their formation. Fractures with similar relative age, size and orientation are observed in 2nd order detachment folds elsewhere in the northeastern Brooks Range (Hanks et al., 1997, 2002; Brinton, 2002; Shackleton, 2003). Because of their regional distribution in both folded and horizontal strata, their orientation sub-perpendicular to the range front, and their age pre-dating fold-related set 2 fractures, these fractures are interpreted to be regional tectonic fractures that formed prior to folding (e.g., Hancock and Engelder, 1989; Engelder and Lacazette, 1990; Lorenz et al., 1991; Engelder and Fischer, 1996).

5.2.2. Syn-folding

Set 2 fractures strike parallel to subparallel to the fold axes and either overprint or are overprinted by fold-related structures. Set 2 fractures are interpreted to have formed as a result of inner- and outer-arc tangential longitudinal strain (TLS) during fold buckling (Fig. 10). Those fractures at a high-angle to bedding are interpreted to have formed due to outer-arc extension; those parallel or at a low-angle to bedding are interpreted to have formed due to inner-arc shortening.

However, set 2 fractures of both orientations occur throughout the fold and do not consistently truncate against bedding, or even the same mechanical unit or subunit boundaries. This suggests that lithologic bedding was not the important mechanical layer during buckling. If it was, fractures would have consistently terminated on bedding surfaces. Instead,

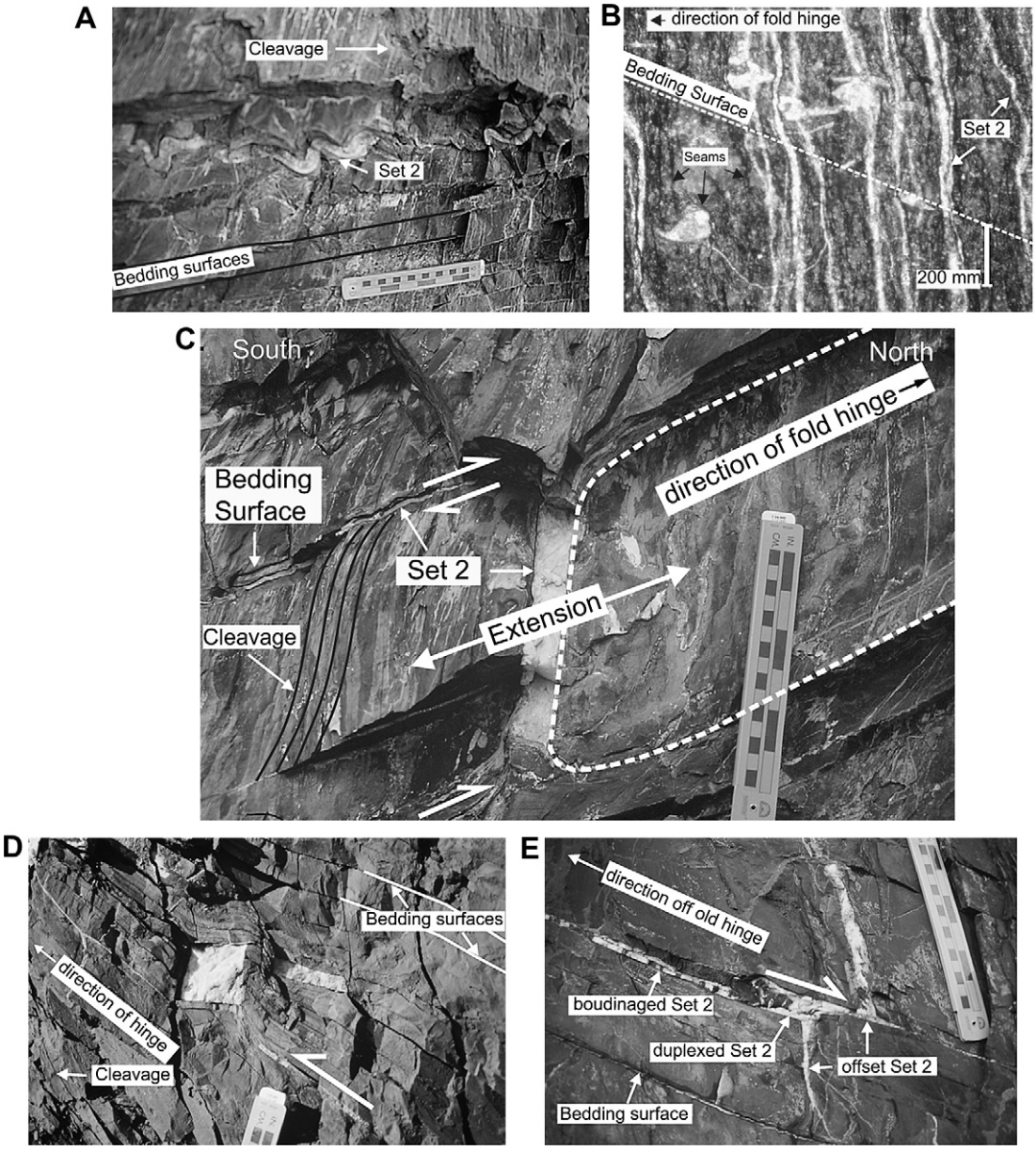

Fig. 9. Photos of mesoscopic and microscopic structures. North is to right in all photos. (A) Spaced cleavage and parasitic folding of layer-parallel, set 2 filled fracture in subunit f in the hinge of fold. (B) Photomicrograph of pervasive dissolution in the mudstone of unit f. Dissolution seams are the black anastomosing lines parallel to the calcite-filled fractures. Set 2 fractures and bioclasts have been dissolved along the seams. (C) Photo of subunit f on south limb of the fold illustrating evidence for early layer-parallel compression followed by layer-parallel extension and late layer-parallel shear toward the hinge. Early cleavage is confined to bedding and deformed by extension. Extension is perpendicular to a wide (~2 cm) calcite filled set 2 fracture and interpreted to be contemporaneous with fracture development. Late top-to-north shear deforms the early cleavage and folds bedding-parallel set 2 calcite-filled fractures. (D) Rotated calcite-filled rhomb, top-to-south shear rotation. Calcite rhomb probably originated as a set 2 fracture that was subsequently boudinaged. Bedding and cleavage are also sheared. (E) Top-to-north-offset of bed-perpendicular set 2 fractures along bed-parallel set 2 fractures. The bed-parallel fractures are themselves both duplexed and extended.

set 2 fractures terminate on mechanical unit and subunit boundaries, implying that these surfaces were the important interfaces during deformation. The fact that set 2 fractures do not consistently occur in a particular part of a mechanical layer or terminate on a particular mechanical unit or subunit boundary implies that the mechanical boundaries changed during progressive folding.

The latest, most vertically extensive set 2 fractures are interpreted to have formed when the fold locked, flexural slip between the mechanical units ceased and the stratigraphy once more acted as one mechanical unit. These large fractures were later sheared during homogeneous flattening in the incompetent Unit 2, and subsequently laterally offset by post-flattening flexural slip along a limited number of bedding surfaces.

5.2.3. Post-folding

Set 3 and 4 fractures are interpreted to post-date folding and, as such, yield no direct information about folding. Both fracture sets are unfilled and are consistently perpendicular

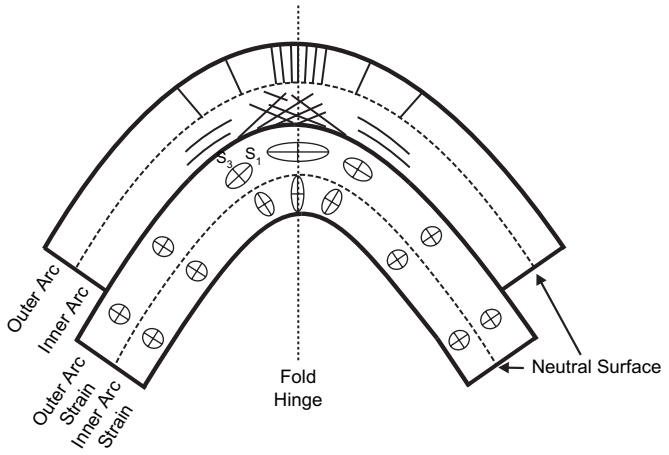

Fig. 10. Tangential longitudinal strain (TLS) associated with buckling of mechanically competent beds. The lower bed illustrates strain distribution in the inner and outer arc separated by a neutral surface. The upper bed illustrates how fracturing can accommodate strain, with extensional fractures in the outer arc and low-angle shear fractures and layer-parallel extensional fractures in the inner arc.

to bedding. Set 3 fractures parallel the fold hinge and terminate against bedding planes, with fracture spacing varying as a function of lithology and bed thickness. These fractures are seen elsewhere in the northeastern Brooks Range, where their spacing also varies with structural position and interlimb angle (Brinton, 2002). The origin of set 3 fractures is poorly constrained, but the lack of mineral fill suggests they formed at shallow depths and in the absence of mineralizing fluids, with fracture spacing and vertical extent more dependent on the host lithology than the mechanical layer.

Set 4 fractures post-date the majority of set 3 fractures, are perpendicular to the fold hinge and sub-perpendicular to the regional thrust front. These fractures are vertically extensive, crossing multiple bed and mechanical unit boundaries, suggesting that mechanical subunits were not active during their formation. Fractures of similar age and character occur throughout the northeastern Brooks Range and are interpreted to be ''unloading'' or ''neotectonic'' joints (Engelder, 1985; Hancock and Engelder, 1989) caused by the contemporary tectonic stress field during denudation, or by existing weakness in the rock fabric.

6. Kinematic model

6.1. Stage 1

In Stage 1 (Fig. 11A) the beds are flat-lying during regional burial. The lithostatic load initially causes vertical compaction and the formation of bedding-parallel stylolites (stress state a). Increased pore fluid pressure combined with low-magnitude differential stress related to the northward prograding fold-and-thrust belt to the south eventually causes regional extension fractures to develop orthogonal to the advancing thrust front (stress state b). Flattened peloids with S_1 perpendicular to bedding and S_3 parallel to bedding within some of the muddier layers indicate that layer-parallel shortening occurred prior to folding, possibly before lithification was complete.

The depth at which this early fracturing occurred is unknown in this particular fold, but fluid inclusion microthermometry from similar fractures in detachment folded Lisburne carbonates from elsewhere in the northeastern Brooks Range suggest the fractures filled at 100–150 °C, corresponding to a depth of ~3–5 km (assuming a geothermal gradient of 30 °C/km) (Hanks et al., 2006).

6.2. Stage 2

Stage 2 (Fig. 11B) represents the onset of folding by flexural slip. Slip occurs along the boundaries between the mechanical units 1, 2 and 3, causing these relatively thick mechanical units to fold with large interlimb angles (180–155°). The mechanical boundaries coincide with significant competency contrasts (i.e., muddy vs. grainy lithologies). Set 2 fractures develop within these thick mechanical units in response to outer and inner arc TLS in each unit. These early, set 2 extension fractures are vertically extensive, crossing multiple bed boundaries that will eventually become subunit boundaries.

6.3. Stage 3

In Stage 3 (Fig. 11C), folding has progressed so that the interlimb angle has decreased to 130°. As layer-parallel strain increases, new slip horizons become active. Slip horizon spacing decreases and thinner mechanical subunits form. Layer-parallel (set 2) fractures develop along these slip horizons.

The new mechanical boundaries put new constraints on fold deformation and the distribution of fractures and other mesoscopic structures. Set 2 fractures continue to form by TLS within the newly developed thinner mechanical subunits. Previously existing, more vertically extensive set 2 fractures formed during stage 2 are laterally offset along new slip horizons.

Each mechanical subunit has both inner and outer arc TLS. At this stage, the interlimb angle is still large (≥130°), so inner arc features are not prevalent in every mechanical subunit. Flexural slip is still the primary deformation behavior during folding and the units maintain constant bed thickness across the fold hinge.

6.4. Stage 4

In Stage 4 (Fig. 11D), the fold has reached an interlimb angle of ~115°. At this stage, flexural slip ceases and the fold is ''locked.'' Direct evidence for this stage is the presence of late-forming, calcite-filled, large set 2 extension fractures that vertically crosscut all of the exposed mechanical subunits, implying that subunits a-m were acting as a single mechanical unit.

The angle of lock-up, or ''critical interlimb angle'', is determined by the frictional properties of the material separating the competent layers (Ramsay, 1974). A critical interlimb

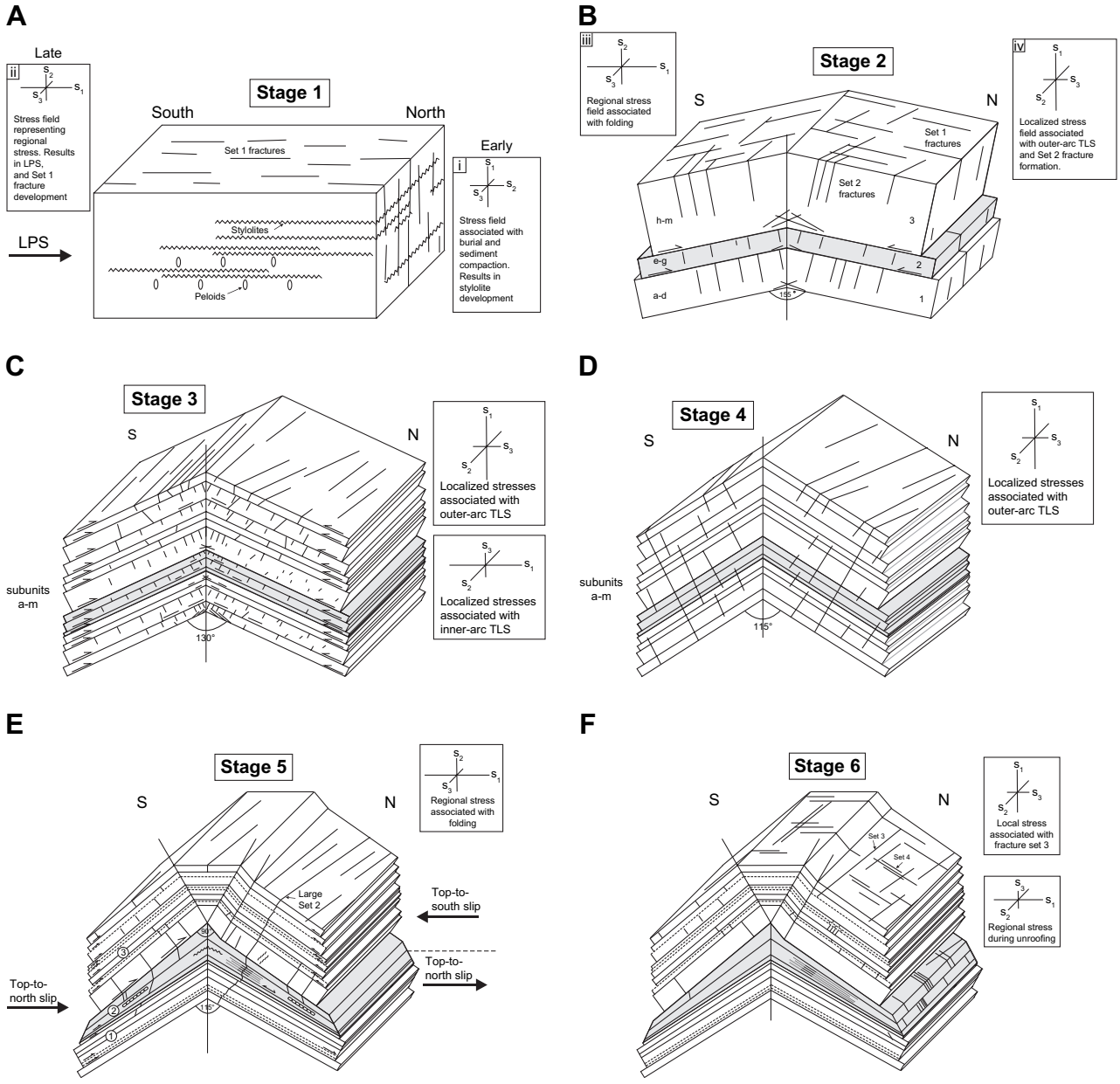

Fig. 11. Kinematic model of fold development. Note that mechanical unit 2 is shaded in B–F. (A) Stage 1: Pre-folding. Stylolites develop in discrete layers due to burial (stress field i). Northward progradation of the northeastern Brooks Range fold-and-thrust belt leads to layer-parallel shortening in the basin sediments (stress field ii). This results in flattened peloids in incompetent horizons and orogen-perpendicular, bed-perpendicular extension fractures (set 1). (B) Stage 2: Early detachment fold development. Widely spaced layer-parallel slip surfaces (indicated by arrows) form between mechanical stratigraphic units 1, 2 and 3. Set 2 extensional fractures within mechanical units 1, 2 and 3 develop due to outer arc extensional tangential longitudinal strain (TLS) (stress state iv); local low-angle set 2 fractures develop due to inner arc compression in lower part of Unit 1. (C) Stage 3: Decrease in slip horizon spacing and mechanical unit thickness as a result of a decrease of the fold interlimb angle. Set 2 fractures continue to form within the newly forming mechanical subunits by TLS. Set 2 fractures from stage 2 (heavier lines) have been offset by newly developed slip horizons. (D) Stage 4: Continued decrease in interlimb angle and fold lock-up. Flexural slip between mechanical subunits ceases and all the stratigraphy acts as a single mechanical unit. The large set 2 fractures form by outer arc extensional TLS of the entire exposed unit thickness and cut through multiple, previously active, subunits. (E) Stage 5. Homogeneous flattening in Unit 2 results in thinning in the limbs and thickening in the hinge. Units 1 and 3 maintain constant thickness. Hinge-planar spaced cleavage, parasitic folds, extensional boudins, and sheared set 2 fractures develop in the incompetent mudstones of Unit 2. No new fractures form during this stage of folding. A secondary detachment surface develops within or along the top contact of the thickened Unit 2, with an associated synclinal hinge in the north limb. (F) Stage 6: Development of post-folding fracture sets 3 and 4 during uplift and erosion.

angle of 115° is nearly twice that proposed by Ramsay (1974). However, the critical interlimb angle in this fold may be partially controlled by mechanical unit thicknesses. Other nearby detachment folds within the lower Lisburne Group have smaller interlimb angles of 70–80°, much closer to the 60° critical interlimb angle proposed by Ramsay (1974). The average mechanical unit thickness in these folds is generally less than that seen in the fold studied here. Other factors that could affect the critical interlimb angle include the thickness of the overall package of rock included in the fold, the thickness of

the underlying incompetent horizon, and/or relative strength of the slip horizons.

6.5. Stage 5

In Stage 5 (Fig. 11E), shortening after fold lock-up is accommodated by homogeneous flattening of the incompetent rocks of Unit 2. Unit 2 thickens in the hinge, with associated parasitic folding of layer-parallel veins and bedding, and development of spaced cleavage. Layer-parallel extension and thinning Unit 2 in the limbs is associated with boudinage of bedding and layer-parallel veins. The large, late-forming, set 2 fractures from stage 4 are sheared and slightly offset in Unit 2.

The entire fold changes geometry due to these thickness changes in Unit 2. In Unit 1 (subunits a–d), the fold geometry remains essentially unchanged with an interlimb angle of ~115°. However, because of hinge thickening, the fold in the overlying Unit 2 (subunits e and g) has an inner arc interlimb angle (115°) greater than that of the outer arc (~90°). The fold in the overlying Unit 3 (subunits h–m) has an interlimb angle of ~90° due to this change in geometry of Unit 2.

A bifurcating synclinal hinge develops in the north limb during this stage with associated calcite-filled, en echelon set 2 fractures. This syncline may be the result of the thickness changes in Unit 2. Alternatively, the synclinal hinge may reflect development of a secondary detachment surface in Unit 2 with some northward translation. Minor northward translation within both Unit 1 and Unit 2 is supported by top-to-the-north offset and shear of set 2 fractures in both units in both the north and south limbs. A small amount of additional shortening by flexural slip occurred within Unit 3, with top-to-north shear in the south limb and top-to-south in the north limb.

6.6. Stage 6

In stage 6 (Fig. 11F), folding has ceased and regional uplift and erosional unroofing has commenced. Extension fractures develop in two orientations. Set 3 fractures form first and are oriented sub-parallel to the fold hinge and sub-perpendicular to bedding. Set 4 fractures form after set 3 fractures, either as a result of in-situ regional stress and/or reactivation of earlier fractures with similar orientation (i.e., set 1).

7. Discussion

7.1. Role of mechanical stratigraphy in detachment folding

In most models of detachment folds, mechanical stratigraphy is a simple system—a mechanically rigid layer abruptly overlying an incompetent layer (e.g, Fig. 1; Jamison, 1987; Homza and Wallace, 1995; Atkinson and Wallace, 2003). However, in many naturally occurring detachment folds the transition between the competent and incompetent units is gradational and/or stratigraphically complex. This study suggests that in these situations, mechanical stratigraphy itself can change during folding, resulting in changes in fold geometry and fold mechanism as shortening increases.

The primary factors influencing the geometry of the third-order detachment folds in the lower Lisburne are the thickness and competency of mechanical stratigraphic units (Homza and Wallace, 1995; Atkinson and Wallace, 2003). Mechanical unit thickness is controlled by the location of major slip horizons. However, this study indicates that mechanical unit boundaries do not always coincide with stratigraphically- or lithologically-defined units—lithostratigraphic units can be grouped into larger mechanical units or, under the right conditions, be divided into smaller mechanical units.

In this study, a decrease in interlimb angle correlated with a decrease in mechanical unit thickness. This suggests that mechanical stratigraphy is not static—mechanical unit thickness can change with increased shortening, as bedding surface strain increases and new slip surfaces form. Consequently, it is difficult to say whether mechanical unit thickness controls interlimb angle or interlimb angle controls mechanical unit thickness.

The thickness and relative competency of mechanical units also influences deformational behavior, fold kinematics and the resulting fold geometry. Units 1 and 3 consist of competent carbonate lithologies with many potential discrete internal slip horizons. Consequently, these two units tended to buckle by flexural slip until the interlimb angle decreased to the point of lock-up. In contrast, Unit 2 consists almost entirely of incompetent calcareous mudstones. While Unit 2 initially may have deformed by flexural slip or flexural flow, after lock-up it continued to deform by homogeneous flattening, with a resulting change in unit thickness from limb to hinge. This change in deformational behavior in Unit 2 resulted in disharmony in the fold geometry.

The mechanical stratigraphy also influences the distribution, character and relative age of fractures and other structures related to folding. During buckling, flexural slip and associated tangential longitudinal strain in the competent units produces extensional structures in the outer arc, and contractional structures in the inner arc. During fold tightening and thinning of the mechanical units, the location of the inner and outer arc and the neutral surface changes as new and thinner mechanical units continue to fold, with resulting structures overprinting earlier structures. This process can go through several iterations, creating fracture and other structure patterns that are difficult to attribute to either the lithostratigraphy or the fold geometry alone. As a consequence, the resulting fracture patterns do not have a clear or simple relationship to the final fold geometry. However, with careful documentation, the relationship between lithostratigraphy, mechanical stratigraphy, fracturing and final fold geometry yields information regarding fold kinematics in a complex stratigraphy.

8. Conclusions

The evolution of detachment folds in the lower Lisburne Group of the northeastern Brooks Range involved an interplay

between lithostratigraphy, mechanical stratigraphy and shortening. A complex lithostratigraphy led to a mechanical stratigraphy that evolved during deformation, with mechanical units becoming thinner as the fold tightened. Changing thickness of the mechanical stratigraphic layers resulted in spatially and temporally overlapping fractures and other mesoscopic structures whose characteristics and distribution were controlled in large part by the thickness and composition of the host mechanical unit.

The deformational behavior also changed with folding depending upon the mechanical stratigraphy. During the early phases of folding and small amounts of shortening, flexural slip along discrete bedding surfaces dominated in mechanical units comprised of thick-bedded, competent lithologies. In contrast, flexural flow dominated in mechanical units composed of thinner bedded, incompetent lithologies. In both instances, the thickness of mechanical units or lithologic beds did not change.

However, flexural slip and flexural flow ceased when the fold reached an interlimb angle of $\sim 90^{\circ}$. After this point, folding continued via homogeneous flattening in the incompetent mechanical unit. This unit thickened in the hinge and thinned in the limbs, resulting in a change in the structural geometry above the unit, but not affecting the geometry of the underlying units. The result was a geometrically disharmonic fold that exhibited characteristics of both buckling and homogeneous flattening.

Acknowledgments

This work benefited greatly from discussions with the various geoscientists that work, or have worked in northern Alaska, especially W. Wallace, M. Whalen, J. Lorenz, J.R. Shackleton, J. Jensen and numerous other graduate students. Reviews by W. Dunne, R. Groshong and an anonymous reviewer were particularly helpful. Financial support was provided by DOE (DE-AC26-98BC15102), BP Alaska, ConocoPhillips. the UAF Graduate School and the Geological Society of America.

References

Atkinson, P.K., 2001. A Geometric Analysis of Detachment Folds in the Northeastern Brooks Range, Alaska, and a Conceptual Model for Their Kinematic Evolution. M.S. thesis, University of Alaska, Fairbanks.

Atkinson, P.K., Wallace, W.K., 2003. Competent unit thickness variation in detachment folds in the northeastern Brooks Range, Alaska: geometric analysis and a conceptual model. Journal of Structural Geology 25, 1751–1771.

Bird, K.J., Molenaar, C.M., 1987. Stratigraphy of the northern part of the Arctic National Wildlife Refuge, northeastern Alaska. In: Bird, K.J., Magoon, L.B. (Eds.), Petroleum Geology of the Northern Part of the Arctic National Wildlife Refuge, Northeastern Alaska, U.S.. Geological Survey Bulletin, 1778, pp. 37–59.

Brinton, J., 2002. Natural Fracturing in Carbonate Rocks as a Function of Lithology and Structural Position in a Detachment Fold: Examples from the Northeastern Brooks Range, Alaska. M.S. thesis, University of Alaska, Fairbanks.

Davis, G.H., Reynolds, S.J., 1996. Structural Geology of Rocks and Regions, second ed. John Wiley and Sons, New York.

Engelder, T., 1985. Loading paths to joint propagation during a tectonic cycle: an example from the Appalachian Plateau. U.S.A. Journal of Structural Geology 7, 459–476.

Engelder, T., Fischer, M.P., 1996. Loading configurations and driving mechanisms for joints based on the Griffith energy-balance concept. Tectonophysics 256, 253–277.

Engelder, T., Lacazette, A., 1990. Natural hydraulic fracturing. In: Barton, Stephansson (Eds.), Rock Joints. A.A. Balkema, Rotterdam, Netherlands, pp. 35–43.

Epard, J.L., Groshong, R.H., 1995. Kinematic model of detachment folding including limb rotation, fixed hinges and layer-parallel strain. Tectonophysics 247, 85–103.

Fischer, M.P., Jackson, P.B., 1999. Stratigraphic controls on deformation patterns in fault-related folds: a detachment fold example from the Sierra Madre Oriental, northeast Mexico. Journal of Structural Geology 21, 613–633.

Gutierrez-Alonso, G., Gross, M.R., 1999. Structures and mechanisms associated with the development of a fold in the Cantabrian Zone thrust belt, NW Spain. Journal of Structural Geology 21, 653–670.

Hancock, P.L., Engelder, T., 1989. Neotectonic joints. Geological Society of America Bulletin 101, 1197–1208.

Hanks, C.L., Lorenz, J., Teufel, L., Krumhardt, A.P., 1997. Lithologic and structural controls on natural fracture distribution and behavior within the Lisburne Group, northeastern Brooks Range and North Slope subsurface, Alaska. American Association of Petroleum Geologists Bulletin 81, 1700–1720.

Hanks, C.L., Wallace, W.K., Lorenz, J.C., Atkinson, P.K., Brinton, J., Shackleton, J.R., 2002. Timing and character of mesoscopic structures in detachment folds and implications for fold development - an example from the northeastern Brooks Range, Alaska. Department of Energy Annual Report. DE-AC26–98BC15102.

Hanks, C.L., Wallace, W.K., Atkinson, P.K., Brinton, J., Bui, T., Jensen, J., Lorenz, J., 2004. Character, relative age and implications of fractures and other mesoscopic structures associated with detachment folds: an example from the Lisburne Group of the northeastern Brooks Range, Alaska. Bulletin of Canadian petroleum Geology 52, 121–138.

Hanks, C.L., Parris, T., Wallace, W.K., 2006. Fracture paragenesis and microthermometry in Lisburne Group detachment folds: implications for the thermal and structural evolution of the northeastern Brooks Range, Alaska. AAPG Bulletin 90 (1), 1–20.

Homza, T.X., Wallace, W.K., 1995. Geometric and kinematic models for detachment folds with fixed and variable detachment depths. Journal of Structural Geology 17, 575–588.

Homza, T.X., Wallace, W.K., 1997. Detachment folds with fixed hinges and variable detachment depth, northeastern Brooks Range, Alaska. Journal of Structural Geology 19, 337–354.

Ismat, Z., Benford, B.A., 2007. Deformation in the core of a fold: unravelling the kinematic evolution of tight, multilayer folds developed in the upper crust. Journal of Structural Geology 29, 497–514.

Jamison, W.R., 1987. Geometric analysis of fold development in overthrust terranes. Journal of Structural Geology 9, 207–219.

Ladeira, F.L., Price, N.J., 1981. Relationship between fracture spacing and bed thickness. Journal of Structural Geology 3, 179–183.

Latta, D.K., Anastasio, D.J., 2007. Multiple scales of mechanical stratification and decollement fold kinematics, Sierra Madre Oriental foreland, northeast Mexico. Journal of Structural Geology 29, 1241–1255.

LePain, D.L., 1993. Transgressive Sedimentation in Rift-flank Region: Deposition of Endicott Group (Early Carboniferous), Northeastern Brooks Range, Alaska. Ph.D. thesis, University of Alaska, Fairbanks.

Lorenz, J.C., Teufel, L.W., Warpinski, N.R., 1991. Regional fractures I: mechanism for the formation of regional fractures at depth in flat-lying reservoirs. American Association of Petroleum Geologists Bulletin 75, 1714–1737.

Moore, T.E., Wallace, W.K., Bird, K.J., Karl, S.M., Mull, C.G., Dillon, J.T., 1994. The Geology of Alaska. In: The Geology of North America. Geological Society of America, Boulder, CO, G1, pp. 49–140.

Narr, W., Suppe, J., 1991. Joint spacing in sedimentary rocks. Journal of Structural Geology 13, 1037–1048.

Poblet, J., McClay, K., 1996. Geometry and kinematics of single-layer detachment folds. American Association of Petroleum Geologists Bulletin 80, 1085–1109.

Price, N.J., Cosgrove, J.W., 1990. Analysis of Geologic Structures. Cambridge University Press, New York.

Ramsay, J.G., 1974. Development of chevron folds. Geological Society of America Bulletin 85, 1741–1754.

Ramsay, J.G., Huber, M.I., 1987. The Techniques of Modern Structural Geology, vol. 2: Folds and Fractures. Academic Press, London.

Shackleton, J.R., 2003. The Relationship between Fracturing, Asymmetric Folding, and Normal Faulting in Lisburne Group Carbonates: West Porcupine Lake Valley, Northeastern Brooks Range, Alaska. M.S. thesis, University of Alaska, Fairbanks.

Tanner, P.W., 1989. The flexural-slip mechanism. Journal of Structural Geology 11, 635–655.

Twiss, R.J., Moores, E.M., 1992. Structural Geology. Freeman, New York.

Wallace, W.K., 1993. Detachment folds and a passive roof duplex: examples from the northeastern Brooks Range. In: Solie, D.N., Tannian, F. (Eds.), Short Notes on Alaskan Geology 1993: Alaska Division of Geologic and Geophysical Surveys Professional Report 113, pp. 81–99.

Wallace, W.K., 2001. Detachment folds and their truncation by thrust faults. United States Department of Energy. First annual report (DE-AC26–98BC15102).

Wallace, W.K., Hanks, C.L., 1990. Structural provinces of the northeastern Brooks Range, Arctic National Wildlife Refuge, Alaska. American Association of Petroleum Geologists Bulletin 74, 1100–1118.

Yang, X., Gray, D.R., 1994. Strain, cleavage and microstructure variations in sandstone: implications for stiff layer behaviour in chevron folding. Journal of Structural Geology 16 (10), 1353–1365.